Do size and shape matter? Exploring the interactions and the metabolome of the soil isolate *Hylemonella gracilis*

Olaf Tyc[1,2*], Purva Kulkarni[1,3], Adam Ossowicki[1], Vittorio Tracanna[4], Marnix H. Medema[4], Peter van Baarlen[5], W.F.J. van Ijcken[6], Koen J. F. Verhoeven[1] and Paolina Garbeva[1, 7]

[1]Netherlands Institute of Ecology (NIOO-KNAW), Department of Microbial Ecology, PO BOX 50, 6700 AB Wageningen, Netherlands

[2]Goethe University, Department of Internal Medicine I, University Hospital Frankfurt, Theodor-Stern-Kai 7, 60590 Frankfurt, Germany

[3]Translational Metabolic Laboratory, Radboud University Medical Center, Geert Grooteplein zuid 10, 6525 GA Nijmegen, Netherlands

[4]Wageningen University, Department of Plant Sciences, Bioinformatics Group, Droevendaalsesteeg 1, 6708 PB Wageningen, Netherlands

[5]Wageningen University, Department of Animal Sciences, Host-Microbe Interactomics, Postbus 338, 6700 WD Wageningen, Netherlands

[6]Center for Biomics, Erasmus University Medical Center, Building Ee, Room Ee6.79b Wytemaweg 80, 3015 CN Rotterdam Rotterdam, Netherlands

[7]Department of Plant and Environmental Sciences, Faculty of Natural and Life Sciences, University of Copenhagen, Denmark

Correspondence:
Goethe University, Department of Internal Medicine I, University Hospital Frankfurt, Theodor-Stern-Kai 7, 60590 Frankfurt, Germany, E-Mail: olaf.tyc@kgu.de

Conflict of Interest Statement

The authors declare that the research was conducted in the absence of any commercial or financial relationships that could be construed as a potential conflict of interest.

Keywords: Small soil bacteria; *Hylemonella* sp.; Interspecific interactions; Volatile-organic-compounds; Transcriptome analysis; Metabolome analysis

Abstract

Microbial community analysis of aquatic environments showed that an important component of microbial diversity consists of bacteria with cell sizes smaller than ~0.1 µm. However, so far no study investigated if such bacteria with small cell sizes exist in terrestrial environments as well.

Here, we isolated soil bacteria that passed through a 0.1 µm filter, by applying a novel isolation and culturing approach. The complete genome of one of the isolates was sequenced and the bacterium was identified as *Hylemonella gracilis*. We performed a set of interaction assays with phylogenetically distant soil bacteria with larger cell and genome size. The interaction assays revealed that *H. gracilis* grows better when interacting with other soil bacteria like *Paenibacillus* sp. AD87 and *Serratia plymuthica*. Furthermore, we observed that *H. gracilis* is able to change the behavior of interacting bacteria without direct cell-cell contact. Transcriptomics and metabolomics analysis was performed with the aim to explain the mechanisms of these interactions.

Our study indicates that soil bacteria that can pass through a 0.1 µM filter may have been overlooked in soil microbial communities and that such bacteria are able to induce transcriptional and metabolomics responses in other soil-bacteria. Furthermore, we revealed that the interaction allowed utilization of substrates that are not utilized by monocultures.

Introduction

Bacteria are ubiquitous living organisms with various cell shapes and sizes surrounding us in all environments (1, 2). Soil is the most complex habitat harboring the largest diversity and density of bacteria known to date (cell densities ranging from 10^7 to 10^{10} cells/g of soil (3-5). Soil bacteria are part of a community where they are in constant interaction with their own and other species (6-8). Bacteria produce and release a plethora of metabolites into their environment. In this way, they not only modify their niche but also affect the behavior and the secondary metabolite production of nearby bacteria (9-11). Soil bacteria are known to produce both soluble and volatile secondary metabolites with different physicochemical and biological properties (7, 12-14). In contrast to soluble compounds, volatile organic compounds (VOCs) are rather small molecules (< 300 Da) that can diffuse easily through air- and water-filled soil-pores, (15-17). These physiochemical properties make VOCs ideal metabolites for long-distance communication and interactions between soil microorganisms (18-21).

In aquatic environments, bacteria are naturally found at lower cell density of 10^3 - 10^6 cells/mL (22-24). Recent studies have shown that a significant component of microbial diversity consists of bacteria with cell sizes smaller than ~0.1 µm (25-27). However, little is known about bacteria with such small cell sizes in soil environments. One can assume that small cell size can be an advantage in challenging environments like soil. The distribution of microorganisms in soil is influenced by its water and moisture content, a low soil moisture content leads to lower connectivity between soil pores, and thus to a lower number of accessible micro-habitats.

Small bacterial cell size is often linked to a small genome size caused by genome streamlining (28). Recent metagenomics studies suggest that genome streamlining is ubiquitous in many bacteria (29, 30). In some cases, the primary metabolism of one organism can be directly built on the primary metabolism of another organism, known as syntrophic relationships (31, 32). The Black Queen Hypothesis states that genome-streamlined organisms have an evolutionary advantage because of the loss of genes whose function can be replaced by bacteria in the surrounding environment, effectively conserving energy (33). Since bacteria with smaller genomes have less adaptive capacity compared to bacteria with bigger genome sizes, many of them depend on specific environmental conditions and the presence of other specific organisms (34) to produce metabolites that support their persistence.

Here, we explore if soil bacteria that are able to pass through 0.1 µm filters are present in soil and we investigated their interaction with other soil bacteria. The major research questions were if, and how inter-specific interactions between bacteria smaller than 0.1 µM and other common

103 soil bacteria affected fitness, behavior, gene expression, and the production of secondary
104 metabolites.
105

106 Materials and Methods

107 Isolation and identification of bacteria that pass through 0.1 µm filters

108 Please see **Fig. S1** and Supplementary Methods.
109

110 Identification of bacteria that passed through 0.1 µm filter

111 One type of bacterial colony was observed on the inoculated plates. The grown colonies were
112 later identified as *Hylemonella gracilis* by 16S rRNA sequence analysis. Please see
113 Supplementary Methods.
114

115 Bacteria and culture conditions

116 Please see Supplementary Methods and **Supplementary Table 1**.
117

118 Microscopy

119 Please see Supplementary Methods.
120

121 Bacterial interactions assays on 1/10th TSBA plates

122 For the interaction assay, liquid bacterial cultures were diluted to an OD_{600} of 0.005
123 (*Paenibacillus* and *Serratia*) or to an OD_{600} of 0.05 (*H. gracilis*). A 10 µl droplet was added in
124 the middle of a 6 cm diameter Petri dish (monocultures) or next to each other in a distance of
125 ~0.5 cm (pairwise interactions), for details please see Supplementary Methods.
126

127 Effects of cell-free supernatants of *Paenibacillus* and *Serratia* on the growth of *H. gracilis*

128 Please see Supplementary Methods.
129

130 DNA isolation and genome sequencing of *H. gracilis*

131 Genomic DNA of *H. gracilis* was extracted using a QIAGEN Genomic-tip 500/G DNA kit
132 Qiagen, cat# 10262 (for details see Supplementary Methods). The genome sequencing was
133 performed on the PacBio RS II platform (Pacific Biosciences, Menlo Park, CA, USA) using
134 P6-C4 chemistry at the Institute for Genome Sciences (IGS), Baltimore, Maryland, USA. The
135 sequencing resulted in a total of 70,101 reads with N50 of 17 309 nucleotides. The PacBio raw
136 sequences were analyzed using SMRT portal V2.3.0.140936. p.4150482. Sequences were

137 assembled *de novo* with the RS_HGAP_assembly 3 protocol (© Copyright 2010 - 2014, Pacific
138 Biosciences, Menlo Park, CA, USA) with default settings on an estimated genome size of 3.8
139 Mbp. The resulting assemblies were subjected to scaffolding using the RS_AHA_scaffolding
140 1 protocol. The genome assembly properties are shown in **Supplementary Table 2**. The final
141 contigs were annotated using PROKKA V1.11 (42) and InterproScan 5.16 55.0 (43). The
142 whole genome sequence was submitted as *Hylemonella gracilis* strain NS1 to NCBI GenBank
143 (https://www.ncbi.nlm.nih.gov/genbank/) under accession # CP031395.
144
145 ***In silico* analysis of secondary metabolite gene clusters**
146 For *in silico* analysis of secondary metabolite gene clusters, the genome sequences of *H.*
147 *gracilis, Paenibacillus sp.* AD87 and *Serratia plymuthica* PRI2C were submitted to the
148 antiSMASH web server (http://antismash.secondarymetabolites.org/) version 4.0 (44).
149
150 **RNA sampling, isolation and RNA- sequencing**
151 Please see Supplementary Methods.
152
153 **Pathway annotations**
154 Please see Supplementary Methods.
155
156 **Exploration of missing genes and genome streamlining in *Hylemonella***
157 RAST annotations of *Serratia*, *Paenibacillus* and *H. gracilis* were used to compare the genomes
158 and to explore the genomes for missing genes in metabolic pathways (http://rast.nmpdr.org)
159 (52-54). RAST was used to identify missing core genes in genomes. The missing gene
160 sequences were extracted and assigned with KEGG Orthology (50, 55). Presence/absence of
161 genes belonging to metabolic pathways was compared across the three genomes to identify
162 shared genes and pathways and to determine incomplete metabolic pathways in *H. gracilis*.
163
164 **Catabolic profiling using BioLog EcoPlate™**
165 Please see Supplementary Methods.
166
167 **Trapping of volatile organic compounds and GC-Q-TOF analysis**
168 Please see Supplementary Methods.
169
170

171 **Ambient mass-spectrometry imaging analysis (LAESI-MSI)**
172 Please see Supplementary Methods.
173
174 **Analysis of Ambient mass-spectrometry imaging (LAESI-MSI) Data**
175 Please see Supplementary Methods.
176
177 **Data availability**
178 The raw data of this article will be made available by the authors, to any qualified researcher.
179 The whole genome sequence of *Hylemonella* strain NS1 is available at the NCBI GenBank
180 under accession # CP031395, the raw reads of the transcriptomics data are available at the
181 Sequence Read Archive (SRA) https://www.ncbi.nlm.nih.gov/sra under accession #
182 PRJNA483535.
183
184 ## Results
185 **Isolation and identification of bacteria that pass through 0.1 µM filter**
186 Using a novel bacterial isolation and cultivation approach, we isolated bacteria from a terrestrial
187 soil sample able to pass through a 0.22 µm and a 0.1 µm pore-size filters. The bacteria were
188 identified as *Hylemonella gracilis* (Gram-negative, class betaproteobacteria, order
189 Burkholderiales). The colonies showed a round and colorless morphology when grown on
190 1/10th TSBA plates (**Fig. 1a**). Microscopically the bacteria had a spiraled morphology with a
191 length of approximately 6 - 12 µM which is typical for *Hylemonella* species (**Fig. 1b**).
192
193 ***Hylemonella* grows better in interaction with other bacteria**
194 *H. gracilis* growth was determined during the interaction with two phylogenetically distantly
195 related soil bacteria (*Paenibacillus* sp. AD87 and *Serratia plymuthica* PRI-2C) and compared
196 to that of the monoculture. The bacterial colony forming units of *H. gracilis* (CFU/mL) obtained
197 on 1/10th TSBA plates from monocultures and interactions are summarized in **Fig. 2**. Cell
198 counts of *Paenibacillus* were 7.68 x 10^7 CFU/mL in interaction with *H. gracilis* (**Fig. 2a**).
199 During the interaction with *H. gracilis*, the growth of *Serratia* was significantly negatively
200 affected ($P=0.037$) after five days of incubation by reaching 1.47 x 10^9 CFU/mL compared to
201 the monocultures (**Fig. 2a**).
202 The bacterial colony forming units (CFU) obtained from *H. gracilis* grown in presence of cell
203 free supernatants (CFS) of *Paenibacillus* and *Serratia* are summarized in **Fig. 2b**. *H. gracilis*
204 growth was significantly increased (P=0.011) when growing in presence of cell free

205 supernatants of *Paenibacillus* resulting in higher cell counts compared to the monoculture by
206 reaching 1.10 x 10^6 CFU/mL. In the presence of cell free supernatant from *Serratia, H. gracilis*
207 reached the highest cell counts at 1.72 x 10^6 CFU/mL (P=0.000) after five days of incubation
208 (**Fig. 2b**).
209
210 **Interaction between bacterial species allows use of substrates that are not used in**
211 **monoculture**
212 The catabolic profiling using EcoPlates™ revealed that *Paenibacillus* was able to utilize 11 of
213 the 31 carbon sources in monoculture, *Serratia* and *H. gracilis* were able to utilize 17 and 16
214 carbon sources respectively. Interestingly, three compounds could be utilized only during co-
215 cultivation of *H. gracilis* with one of the other species, these compounds could not be utilized
216 by any of the species in monoculture. Specifically, alpha- cyclodextrin was utilized only during
217 co-cultivation of *H. gracilis* with *Paenibacillus*, while L-threonine and glycyl-L-glutamic acid
218 were utilized only during the interaction of *Serratia* and *H. gracilis* **Fig. 3.**
219
220 **Genomic features of *H. gracilis, Serratia and Paenibacillus***
221 Sequencing of the complete genome of *H. gracilis* resulted in a genome size of 3.82 Mbp with
222 3,648 coding sequences (CDS). As expected, the genome analysis revealed that the genome of
223 *Hylemonella* is smaller and contains fewer genes when compared to both *Serratia plymuthica*
224 PRI-2C (5.4 Mbp) and *Paenibacillus* sp. AD87 (7 Mbp). The genome features of all three
225 bacteria are summarized in **Supplementary Table 2**.
226
227 ***In silico* analysis of gene clusters encoding for secondary metabolites**
228 *In silico* analysis of *Paenibacillus* revealed a total of 10 gene clusters coding for secondary
229 metabolites. From which two gene clusters belonged to the class of terpenes, one to
230 bacteriocins, one to lasso peptides, two to the class of lanthipeptides, one to nonribosomal
231 peptides, one to others, one to the class of type III polyketide synthases and one gene cluster
232 belonging to the class of siderophores (**Fig. 4a**). For *Serratia* the *in silico* analysis revealed in
233 total 9 gene clusters from which two gene clusters belonged to the class of Non-Ribosomal
234 Peptides, one to Hsr-lactones, one to Aryl polyene- Siderophores, one to the class of T1PKS-
235 NRPS hybrids, one to the class of Thiopeptides, one to the class of Butyrolactones, one to the
236 class of Terpenes and one to the class of others (**Fig. 4b**). Flor *H. gracilis* the AntiSMASH
237 analysis revealed that *H. gracilis* possesses relatively few gene clusters related to secondary
238 metabolism. A total of three gene clusters for *H. gracilis* were detected, of which one belonged

239 to the class of bacteriocins, one to the class of terpenes, and one to aryl polyenes, the latter
240 being a homolog to the aryl polyene gene cluster from *Xenorhabdus doucetiae* (Genbank:
241 NZ_FO704550.1) **Fig. 4c**.
242
243 **Pathway analysis in *H. gracilis* compared to *Serratia* and *Paenibacillus***
244 The RAST comparison of *Paenibacillus* and *H. gracilis* revealed that 504 unique enzymes
245 (according to their EC numbers) were exclusive to *Paenibacillus*, while 434 were present only
246 in *H. gracilis*; 532 EC numbers shared by both genomes (**Fig. 5a**). The RAST comparison of
247 *Serratia* and *H. gracilis* revealed that 751 enzymes were present only in *Serratia*, and 260 were
248 present only in *H. gracilis*. 727 EC numbers participating in diverse metabolic pathways were
249 found in both genomes (**Fig. 5b**).
250 The RAST analysis revealed five missing genes in *H. gracilis* compared to *Serratia* and
251 *Paenibacillus*. The missing genes were annotated with the following ontology terms:
252 GO:0008473 (ornithine cyclodeaminase activity), GO:0008696 (4-amino-4-
253 deoxychorismatelyase activity), GO:0003920 (GMP reductase activity), GO:0004035 (alkaline
254 phosphatase activity) and GO:0008442 (3-hydroxyisobutyrate dehydrogenase). We verified if
255 the loss of these genes would render specific pathways obsolete. However, alternative pathways
256 routes are present for these GO terms according to the KEGG database. The pathway analysis
257 by RAST did not suggest any essential missing pathway components in metabolic pathways in
258 *H. gracilis*. Still, the comparison of the number (n) of genes present in each RAST subsystem
259 category revealed major differences in several subsystem categories, specifically in the
260 categories "Carbohydrates metabolism" and "Phosphorus metabolism" (**Fig. 5c**). *H. gracilis*
261 possesses no genes for these categories, whereas *Paenibacillus* possesses 393 and 82 genes,
262 and *Serratia* 395 and 46 genes, respectively. A major difference in the absolute number of genes
263 in a category is also observed for Amino Acids and Derivatives, for which *H. gracilis* possesses
264 318 genes, *Paenibacillus* possesses 358 and *Serratia* 448 genes.
265
266 **Effect of inter-specific interactions on gene expression**
267 RNA- sequencing was performed to better understand the effects of bacterial interaction on
268 gene expression of each interacting partner. The transcriptome analysis of monocultures and
269 interspecies interactions revealed a total of 277 significant differentially expressed genes; 100
270 down-regulated and 177 up-regulated (**Supplementary Table 2**).
271
272

273 *Effect of inter-specific interactions on gene expression in Paenibacillus and H. gracilis*
274 In *Paenibacillus* histidine biosynthesis and dephosphorylation genes were up-regulated
275 (**Supplementary Table 3**), while cellular-growth-related genes were down-regulated
276 (**Supplementary Table 3**) at day 10 of the interaction with *H. gracilis* (**Fig. 6b**). For the
277 interaction of *H. gracilis* with *Paenibacillus* a total of 15 significant differentially expressed
278 genes were found (0 at day 5 and 15 at day ten). At day five, genes related to sulfur assimilation,
279 chemotaxis and response to (chemical/external) stimuli were upregulated in *H. gracilis* in the
280 presence of *Paenibacillus*. Genes related signal transduction (T) were the category with the
281 most differentially expressed genes during the interaction of *H. gracilis* with *Paenibacillus*
282 compared to the monoculture of *H. gracilis* (**Supplementary Table 8** and **9**, **Fig. 6a, b**).
283
284 *Effect of inter-specific interactions on gene expression Serratia and H. gracilis*
285 During the interaction of *Serratia* with *H. gracilis*, 61 genes were significantly differentially
286 expressed at day five and 10 at day ten. At the day five, iron-sulfur cluster-assembly-related
287 genes, a sulfur transferase and a transaminase were up-regulated, while genes related to
288 inorganic diphosphatase activity, exonuclease activity and DNA repair were downregulated. At
289 day ten, genes related to sulfur transmembrane transport, sulfur compound catabolism and
290 cysteine biosynthesis were upregulated, and genes related to sulfur compound metabolism and
291 translation were downregulated. (**Supplementary Table 4** and **5**). For *Serratia*, genes related
292 to signal transduction and translation, ribosome structure and biogenesis were the most
293 differentially expressed gene categories (**Fig. 6c**). For *H. gracilis* in interaction with *Serratia*,
294 182 differentially expressed genes were identified at day ten and only one at day five. At day
295 five, genes related to the ribosome/ribonucleoproteins, organelle organisation/assembly and
296 (iron)-sulfur cluster assembly were upregulated and genes related to the innate immune
297 response (Toll Like Receptor signalling) were downregulated (**Supplementary Table 6** and **7**).
298 At day ten, genes related to signal transduction and chemotaxis were up- regulated in *H.*
299 *gracilis*. For *H. gracilis*, the most upregulated genes were linked to the chemotaxis pathway
300 and iron scavenging, indicating activity in competition (**Fig. 6a**).
301
302 **Metabolomic analysis of volatile compounds**
303 The volatile blend composition of the monocultures differed from that of the co-cultures. Clear
304 separations between the controls, monocultures and co-cultures were obtained in PLS-DA score
305 plots (**Fig. 7a**). The analysis revealed a total of 25 volatile organic compounds produced by
306 mono- and co-cultured bacteria that were not detected in the non-inoculated controls (**Table 2**).

307 Of these, 17 are identified and categorized in six chemical classes (alkenes, benzoids, sulfides,
308 thiocyanates, terpenes, furans). The remaining eight compounds could not be assigned with
309 certainty to a known compound. The most abundant volatile organic compounds were sulfur-
310 containing compounds such as dimethyl disulfide ($C_2H_6S_2$) and dimethyl trisulfide ($C_2H_6S_3$).
311 These two sulfur compounds were produced by all three bacteria. Interestingly an unknown
312 compound with RT 26.4 min produced by the monocultures of *H. gracilis* was not detected in
313 the interactions with *Serratia* (**Table 2**). Two other unknown compounds with RT 4.15 min and
314 with RT 24.34 min produced by the monocultures of *Paenibacillus* were not detected in the
315 interactions with *H. gracilis* (**Table 2**).
316
317 **DART-MS based metabolomics**
318 The metabolomics analysis based on DART-MS revealed separations between the controls,
319 monocultures, and co-cultures as presented in PLS-DA score plots (**Fig. 7b**). The metabolomic
320 composition of the monocultures differed from that of the co-cultures (**Fig. 7b**). Statistical
321 analysis (ONE-WAY ANOVA and post-hoc TUKEY HSD-test) revealed 617 significant mass
322 features present on day five and day ten of which 48 could be tentatively assigned to specific
323 compounds. Most of the significant peaks were found in the co-cultures of *H. gracilis* with
324 *Paenibacillus*. The significant mass features and the corresponding tentative metabolites can
325 be found in **Supplementary Table 10**.
326
327 **Mass spectrometry imaging metabolomics**
328 LAESI-MSI was performed to visualize the localization of metabolites in their native
329 environments in monoculture as well as during interaction without performing any extraction.
330 Across all treatments, clear separation was observed amongst the samples for controls,
331 monocultures and interactions **(Fig. 8a)**. An average of 1050 mass features was detected per
332 treatment. To list mass features that could explain separation amongst the controls,
333 monocultures and interactions, values of variable importance in projection (VIP) were
334 calculated. The top 40 statistically significant mass features with a VIP score > 2.0 are shown
335 in **Fig. 8b**. The mass features have been listed based on their decreasing influence on
336 classification amongst the different treatments. To visualize the statistically significant mass
337 features between monoculture and interaction samples in a pairwise manner, volcano plots were
338 constructed **(Fig. S3)**. Metabolites with a log2 fold change threshold of 1.0 on the x-axis and a
339 t-test threshold (*p* value) of 1.0 on the y-axis were considered significantly differentially
340 abundant between monoculture and interaction samples.

341 The volcano plot (**Fig. S3a**) for *Hylemonella* monoculture (HM) and the interaction of *H.*
342 *gracilis* with *Paenibacillus* (PH) shows 53 mass features (in green) located in the upper right
343 quadrant, indicating that their concentrations are significantly higher in HM as compared to
344 PH. 18 mass features (in red) in the upper left quadrant of the plot have a significantly lower
345 concentration in HM as compared to PH. The box-and-whisker plots for the four statistically
346 significant differentially abundant metabolites selected from the volcano plot for the pair HM
347 and PH are shown in **Fig. S2a**. The ion intensity maps for these statistically significant
348 metabolites are shown alongside box-and-whisker plots. The ion intensity maps are color coded
349 based on the standard rainbow color scale where a pixel in red represented a high concentration
350 and the pixel in black represents no concentration of the selected metabolite. As can be seen,
351 *m/z* 425.2886 and *m/z* 558.2832 show higher abundance in interaction sample PH, whereas *m/z*
352 410.8587 and *m/z* 716.7610 display high abundance in HM as compared to PH.
353
354 For the pairwise analysis performed for *Paenibacillus* monoculture (PM) and the interaction of
355 *H. gracilis* with *Paenibacillus* (PH), 149 mass features (in green) displayed significantly high
356 concentration in PM and 75 mass features (in red) had significantly low concentration in PM
357 as compared to PH (**Fig. S3b**). This is also evident in the box-and-whisker plots and the ion
358 intensity maps that are presented for four statistically significant metabolites belonging to this
359 set (**Fig. S2b)**.
360
361 For the pairwise analysis for *H. gracilis* monoculture (HM) and the interaction of *Serratia* and
362 *H. gracilis* (SH), 57 mass features (in green) displayed significantly high concentration in HM
363 and 42 mass features had significantly low concentration in HM as compared to SH (**Fig. S3c**).
364 The box-and-whisker plots along with the ion intensity maps for four statistically significant
365 metabolites belonging to this set are shown in **Fig. S2c**. For the pairwise analysis for *Serratia*
366 monoculture (SM) and the interaction of *Serratia* and *H. gracilis* (SH), 135 mass features (in
367 green) displayed significantly high concentration in SM and 65 mass features had significantly
368 low concentration in SM as compared to SH (**Fig. S3d**). The box-and-whisker plots along with
369 the ion intensity maps for four statistically significant metabolites belonging to this set are
370 shown in **Fig. S2d**.
371
372 To visualize the number of shared and unique metabolites amongst the monoculture and
373 interaction samples Venn diagrams were plotted. The Venn diagram (**Fig. S3e**) for
374 monocultures *H. gracilis* and *Paenibacillus* and their interaction shows 80 metabolites unique

375 to *H. gracilis* monoculture, 75 metabolites unique to *Paenibacillus* monoculture and 100
376 metabolites that are unique during their interaction. 1062 metabolites were shared within these
377 three treatments. Similarly, the Venn diagram **(Fig. S3f)** for monocultures *H. gracilis* and
378 *Serratia* and their interaction shows 196 metabolites unique to *H. gracilis* monoculture, 48
379 metabolites unique to *Serratia* monoculture and 120 metabolites that are unique during their
380 interaction.
381
382 **Discussion**
383
384 Here we report the first time isolation of *H. gracilis* from a terrestrial soil sample. This
385 bacterium passed a 0.1 µm filter, which suggests a very small cell size, justifying ultra-small
386 bacteria (26). However, against our expectation, the microscopical analysis revealed that this
387 bacterium is not ultra-small in cell size but possesses a very thin diameter and showed the
388 typical spiraled morphology known for these species (63-66). These observations are in line
389 with previous research by Wang et al. showing that *H. gracilis* is capable of passing through
390 filters of various pore sizes ranging from 0.45 µM to 0.1µM (67), most probably thanks to their
391 cell shape and cell morphology.
392 The bacterial interaction assays revealed that H. gracilis grows better when interacting with
393 Paenibacillus sp. Or Serratia. H. gracilis cell numbers were higher when exposed to cell-free
394 supernatants of Paenibacillus and Serratia, suggesting that H. gracilis interaction benefits are
395 related to the metabolites released by these bacteria. We hypothesized that H. gracilis grows
396 better in co-culture, either because growth is stimulated by signals produced by the other
397 organism, or because the environment that is created by the other organism allows H. gracilis
398 to make more efficient use of the metabolic pathways. Indeed, the metabolic experiments with
399 BioLog™ plates showed that during interspecific interactions of H. gracilis with Paenibacillus
400 or with Serratia, more carbohydrates could be utilized compared to the monocultures. This is
401 an interesting observation, as it indicates that the interaction of bacteria can trigger the
402 production of exo-enzymes enabling the degradation of carbohydrates, which the bacteria were
403 not able to degrade in monoculture.
404 We speculated that since *H. gracilis* grows better in interaction with other bacteria and is of
405 relatively small cell size, it is possible that *H. gracilis* has evolved a genome streamlining
406 strategy, i.e. the adaptive loss of genes for which functions it relies on interaction with other
407 bacteria. Indeed, whole-genome sequencing of *H. gracilis* revealed a genome size of 3.82 Mbp.
408 This is a relatively small genome size for free-living soil bacteria that typically have estimated
409 average genome sizes of ~4.7 Mbp (34, 68-71). The *in silico* antiSMASH (44) comparison of

410 genes that are part of secondary metabolite gene clusters showed that the *H. gracilis* genome
411 contained only three gene clusters encoding the production of secondary metabolites
412 (bacteriocins, terpenes, and aryl polyenes), which provides additional evidence of genome
413 streamlining. Terpenes and aryl polyenes are known as protective compounds against abiotic
414 stressors, while bacteriocins have antimicrobial activities against closely related bacteria (17,
415 72-76). We hypothesized that *H. gracilis* has undergone genome streamlining, to be more
416 competitive, by retaining only the most essential metabolic functions. Genome streamlining
417 refers to the reduction of genome size by loss of genes, which may for instance evolve in
418 symbiotic or co-occurring species when some genomic functions are redundant in one species
419 and are functionally compensated by other species (Giovannoni et. al., 2014). Thus, gene loss
420 and reduced genome size may cause dependency on other microbes in their surroundings, and
421 this may explain a considerable part of the phenomenon of the uncultured microbial majority.
422 Interestingly, most of the data supporting streamlining theory come from the study of bacteria
423 from aquatic environments, where bacterial cell density is lower. However, the same process
424 may be important in high density soil microbial communities.
425
426 To understand the mechanisms of interaction, we performed transcriptome analysis on
427 the interaction pairs of *H. gracilis* with *Serratia* and *Peanibacillus*. Interestingly, more
428 significantly differentially expressed genes were induced by *H. gracilis* in the other two
429 competing bacteria as compared to the transcriptomic changes in *H. gracilis* induced by
430 *Serratia* or *Paenibacillus* (**Supplementary Table 2**). Several processes, enriched according to
431 GO term enrichment analysis, could be part of a mechanism(s) mediating interactions between
432 *H. gracilis* and *Serratia* and *Paenibacillus*, for example genes related to chemotaxis. Moreover,
433 the GO terms for signal transduction, secondary metabolite production and, cell motility were
434 enriched in the transcriptome of *H. gracilis* during the interaction with *Paenibacillus*,
435 suggesting that chemotaxis is an important feature during interspecific interactions between
436 these two bacterial taxa (77, 78). In addition, Iron-sulfur (Fe-S) complex assembly GO terms
437 were enriched in the transcriptomes of *H. gracilis* during the interaction with *Serratia* and
438 *Paenibacillus*. Fe-S clusters are important for sustaining fundamental life processes: they
439 participate in electron transfer, substrate binding/activation, iron or sulfur storage, regulation of
440 gene expression, and enzyme activity (80, 81). This up-regulation could indicate that in co-
441 culture, the interacting bacteria releases metabolites that *H. gracilis* could use for synthesizing
442 Fe-S complexes. It is also possible that iron-sulfur complex assembly is activated during
443 competition with the interacting bacteria for sulfur, or iron collection (82-85).

444 The metabolic pathway analysis showed that the loss of genes in *H. gracilis* does not
445 appear to have resulted in functional loss of metabolic pathways. However, shedding non-
446 necessary redundant genes in several metabolic pathways could explain why and how the
447 genome of *H. gracilis* has become so small. Nevertheless, the lost genes are not essential to
448 complete metabolic pathways and only appear to result in limited options in certain metabolic
449 pathways. The RAST analysis showed that all metabolic pathways remain feasible. The only
450 exception is EC term 5.2.1.1 (maleate isomerase) which makes it not clear which alternative
451 pathway can be used by *H. gracilis* to synthesize fumarate. There are several ways to synthesize
452 fumarate, e.g. in the glycolysis pathway (66, 92, 93) and in the citric acid cycle (66, 94). The
453 performed metabolomics analysis revealed the production of specific antimicrobial compounds
454 such as pyrollnitrin (*Serratia*) and 2,5-bis(1-methylethyl)-pyrazine (*Paenibacillus*) which are
455 well known for their broad-spectrum antimicrobial activity (95-99). However, the produced
456 antimicrobial compounds didn't show activity against *H. gracilis*: in both interactions, *H.*
457 *gracilis* showed increased growth when growing in co-culture with either *Paenibacillus* or
458 *Serratia*.
459 The understanding of natural metabolites that mediate interactions between organisms
460 in natural environments is the key to elucidate ecosystem functioning. The detection and
461 identification of the compounds that mediate such interactions is still challenging. Techniques
462 such as mass spectrometry imaging (MSI) provide new opportunities to study environmentally
463 relevant metabolites in their spatial context (35-37). In this study, the metabolomics was
464 performed using three independent approaches namely DART-MS analysis, GC/MS-Q-TOF
465 analysis and, ambient imaging mass spectrometry (LAESI- MS) from living bacterial colonies.
466 The Imaging MS analysis revealed that several mass features were detected in higher abundance
467 during the interaction of *H. gracilis* with *Paenibacillus*, these mass features were m/z 425.2886
468 and m/z 558.2832. However, the here used technology (LAESI-MSI) is not suitable for
469 unambiguous compound annotation, but LAESI- MSI can still be used for putative compound
470 annotation. To annotate the detected mass features to compounds with high certainty, LAESI
471 mass spectrometry imaging should be coupled with ion mobility separation as suggested by
472 (100-102). Yet, LAESI-MSI can help to spatially distinguish the produced secondary
473 metabolites of living bacterial colonies with limited sample preparation and can give insight
474 into the spatial distribution of metabolites.
475 Several studies indicate that the volatile composition of the volatiles greatly depends on biotic
476 interactions and on growth conditions (15, 19, 59, 103, 104). Here, a higher number of volatile
477 compounds were detected in the bacterial interaction pairs, most likely due to the combination

478 of emitted volatiles of the interacting bacteria. The high amount of sulfur-containing
479 compounds indicates that these compounds are commonly produced by bacteria and might play
480 an important role in signaling during interspecific interactions (105, 106). However, no novel
481 volatile compounds during the co-cultivation of the three bacteria were detected.
482 Overall, our study showed that *H. gracilis* is able to pass through 0.1 μM filter, and is present
483 in terrestrial environments. The growth and behavior of *H. gracilis* were dependent on the
484 interacting partner and they might be metabolically dependent on the neighboring bacteria. At
485 the same time, *H. gracilis* is able to change the behaviour of the interacting bacteria without
486 direct cell-cell contact. This study have laid a good bases for isolating soil bacterial with a small
487 cell size and for exploring interactions between bacteria with different cell and genome size.
488 Deciphering such interactions is key to understanding ecosystem functioning and the assembly
489 of microbial communities.
490
491
492 **Acknowledgement**
493 This work was financially supported by The Netherlands Organization for Scientific Research
494 (NWO) VIDI personal grant 864.11.015 granted to PG. The authors also want to thank the
495 students of the WUR bioinformatics course BIF-51806 (2018) for their input and primarily data
496 analysis and discussions on the data.
497
498 **Author contributions**
499 OT and PG designed the experiments. OT, AO, PK and WIJ performed the lab experiments.
500 OT, PK and performed the data analysis and prepared the figures and tables. OT, PK, AO, VT,
501 MHM, PB, KJFV and PG wrote the manuscript.
502
503 **Figure legends**
504 **Figure 1: Microscopy pictures of *Hylemonella gracilis*** (**a**) colonies on agar plates captured
505 at 20x magnification and (**b**) single bacterial cells captured at 400 X magnification.
506
507 **Figure 2: Colony counts (CFU/mL) revealed after 5 days of incubation during the plate**
508 **based interaction experiment (a) and (b) revealed during the cell free supernatant (CFS)**
509 **exposure experiment.** Abbreviations: *H. gracilis* monoculture (HM), *Paenibacillus* sp. AD87
510 monoculture (PM), *Paenibacillus* sp. AD87 – *H. gracilis* coculture (PH), *S. plymuthica*
511 monoculture (SM), *S. plymuthica* - *H. gracilis* coculture (SH). *H. gracilis* - *Paenibacillus* sp.
512 AD87 coculture (HP), *H. gracilis* – *S. plymuthica* coculture (HS). Significant differences in

513 cell counts (CFU/mL) between co-cultures (treatment) and monocultures (controls) are
514 indicated by asterisks (ONE-WAY ANOVA, post-hoc TUKEY test).
515
516 **Figure 3: Results overview of the Biolog EcoPlate^{TM} experiment.** The EcoPlate contains 31
517 different carbon sources, bacteria were inoculated in monoculture or in pairwise combinations.
518 Colour codec: blue=carbon source could be utilized in monoculture, yellow= carbon source
519 could be utilized in co-culture. Abbreviations: *Paenibacillus* sp. AD87 monoculture (PM),
520 *Paenibacillus* sp. AD87 - *H. gracilis* coculture, (PH) *H. gracilis* monoculture (HM), *S.*
521 *plymuthica* PRI-2C monoculture (SM), *S. plymuthica* PRI-2C - *H. gracilis* coculture
522 (SH).
523
524 **Figure 4: *In silio* comparison of biosynthetic gene clusters (BGCs) present in the three soil**
525 **bacteria based on antismash *in silico* analysis** (https://antismash.secondarymetabolites.org/).
526 From left to right (**a**) *Paenibacillus* sp. AD87 with a genome size of 7.0 MBp, n=10 gene
527 clusters for secondary metabolites, (**b**) *S. plymuthica* PRI-2C with a genome size of 5.4 MBp,
528 n=9 gene clusters for secondary metabolites and (**c**) *H. gracilis* with a genome size of 3.8 MBp,
529 n= 3 gene clusters for secondary metabolites.
530
531 **Figure 5:** Results of the comparison analysis carried out with the RAST pipeline
532 (https://rast.nmpdr.org/) (**a**) Venn- diagram showing the results for the number (n) of expressed
533 genes present solely in monoculture and the number of shared expressed genes for the
534 monocultures of *Hylemonella* (HM), *Paenibacillus* monoculture (PM) and *Serratia*
535 monoculture (SM) and the interaction of *Hylemonella* with *Paenibacillus* (PH) and for the
536 interaction of *Hylemonella* with *Serratia* (SH). (**b**) Boxplot showing number (n) of expressed
537 genes present in each RAST subsystem category.
538
539 **Figure 6: Pie-charts representing up-regulated genes identified by differential gene**
540 **expression analysis and COG annotation** (**a**) *Hylemonella gracilis* monoculture gene
541 expression level (**b**) *H. gracilis* in co-culture with *Paenibacillus* sp. AD87; (**c**) *H. gracilis* co-
542 culture with *S. plymuthica* PRI-2C. In the co-culture of *H. gracilis* with *Paenibacillus* sp. AD87,
543 genes related to signal transduction (**T**) were the category with the most differentially expressed
544 genes. In the co- culture of *H. gracilis* with *S. plymuthica* PRI-2C genes related to signal
545 transduction (**T**), translation, ribosome structure and biogenesis (**J**) were the most prevalent
546 differentially expressed gene categories.

547 **Figure 7: PLSD-A plots of the metabolomics data** (**a**) PLS-DA 2D- plots of volatiles emitted
548 by monocultures and pairwise combinations of *H. gracilis*, *Paenibacillus* and *Serratia*
549 *plymuthica* after ten days of inoculation, time point (t=10 days) (**b**) PLS-DA 2D- plots of the
550 analysed DART-MS data of monocultures and mixtures of *H. gracilis*, *Paenibacillus* sp. AD87
551 and *Serratia plymuthica* PRI-2C after ten days of inoculation, time point (t=10 days).
552
553 **Figure 8: PLS-DA plots of the first 40 significant mass features observed after analysis of**
554 **the LAESI-MSI data. (a)** PLS-DA score plot for *H. gracilis* monoculture (HM), *Paenibacillus*
555 *sp. AD87* monoculture (PM), *Paenibacillus* sp. AD87 – *H. gracilis* coculture (PH), *S.*
556 *plymuthica* PRI-2C monoculture (SM), *S. plymuthica* PRI-2C - *H. gracilis* coculture (SH) and
557 TSBA control (TSBA). **(b)** First 40 statistically significant features identified by PLS-DA based
558 on Variable Importance in Projection (VIP) score. The colored boxes on the right indicate the
559 relative concentrations of the corresponding metabolite in each group under study.
560

561 ## References

562 1. Gibbons SM, Gilbert JA. 2015. Microbial diversity—exploration of natural
563 ecosystems and microbiomes. Current Opinion in Genetics & Development 35:66-
564 72.
565 2. Levin PA, Angert ER. 2015. Small but Mighty: Cell Size and Bacteria. Cold Spring
566 Harbor Perspectives in Biology 7.
567 3. Uroz S, Buee M, Murat C, Frey-Klett P, Martin F. 2010. Pyrosequencing reveals a
568 contrasted bacterial diversity between oak rhizosphere and surrounding soil.
569 Environmental Microbiology Reports 2:281-288.
570 4. Curtis TP, Sloan WT, Scannell JW. 2002. Estimating prokaryotic diversity and its
571 limits. Proc Natl Acad Sci U S A 99:10494-9.
572 5. Torsvik V, Ovreas L. 2002. Microbial diversity and function in soil: from genes to
573 ecosystems. Curr Opin Microbiol 5:240-5.
574 6. Stubbendieck RM, Vargas-Bautista C, Straight PD. 2016. Bacterial Communities:
575 Interactions to Scale. Frontiers in Microbiology 7.
576 7. Hibbing ME, Fuqua C, Parsek MR, Peterson SB. 2010. Bacterial competition:
577 surviving and thriving in the microbial jungle. Nature Reviews Microbiology
578 8:15-25.
579 8. Cornforth DM, Foster KR. 2013. Competition sensing: the social side of bacterial
580 stress responses. Nature Reviews Microbiology 11:285-293.
581 9. Traxler MF, Watrous JD, Alexandrov T, Dorrestein PC, Kolter R. 2013. Interspecies
582 Interactions Stimulate Diversification of the *Streptomyces coelicolor* Secreted
583 Metabolome. Mbio 4(4), e00459-13.
584 10. Tyc O, van den Berg M, Gerards S, van Veen JA, Raaijmakers JM, de Boer W,
585 Garbeva P. 2014. Impact of interspecific interactions on antimicrobial activity
586 among soil bacteria. Frontiers in Microbiology 5,.
587 11. Seyedsayamdost MR, Traxler MF, Clardy J, Kolter R. 2012. Old Meets New: Using
588 Interspecies Interactions to Detect Secondary Metabolite Production in
589 Actinomycetes. Natural Product Biosynthesis by Microorganisms and Plants, Pt C
590 517:89-109.

12. Crits-Christoph A, Diamond S, Butterfield CN, Thomas BC, Banfield JF. 2018. Novel soil bacteria possess diverse genes for secondary metabolite biosynthesis. Nature 558:440-444.
13. Reddy BVB, Kallifidas D, Kim JH, Charlop-Powers Z, Feng ZY, Brady SF. 2012. Natural Product Biosynthetic Gene Diversity in Geographically Distinct Soil Microbiomes. Applied and Environmental Microbiology 78:3744-3752.
14. Charlop-Powers Z, Owen JG, Reddy BVB, Ternei MA, Brady SF. 2014. Chemical-biogeographic survey of secondary metabolism in soil. Proceedings of the National Academy of Sciences 111:3757-3762.
15. Schulz S, Dickschat JS. 2007. Bacterial volatiles: the smell of small organisms. Nat Prod Rep 24:814-42.
16. Kai M, Haustein M, Molina F, Petri A, Scholz B, Piechulla B. 2009. Bacterial volatiles and their action potential. Appl Microbiol Biotechnol 81:1001-12.
17. Tyc O, Song C, Dickschat JS, Vos M, Garbeva P. 2017. The Ecological Role of Volatile and Soluble Secondary Metabolites Produced by Soil Bacteria. Trends in Microbiology 25:280-292.
18. Chernin L, Toklikishvili N, Ovadis M, Kim S, Ben-Ari J, Khmel I, Vainstein A. 2011. Quorum-sensing quenching by rhizobacterial volatiles. Environmental Microbiology Reports 3:698-704.
19. Tyc O, Zweers H, De Boer W, Garbeva P. 2015. Volatiles in inter-specific bacterial interactions. Frontiers in Microbiology 6.
20. Schmidt R, Cordovez V, de Boer W, Raaijmakers J, Garbeva P. 2015. Volatile affairs in microbial interactions. ISME J doi:10.1038/ismej.2015.42.
21. Effmert U, Kalderas J, Warnke R, Piechulla B. 2012. Volatile mediated interactions between bacteria and fungi in the soil. J Chem Ecol 38:665-703.
22. Rocha AM, Yuan Q, Close DM, O'Dell KB, Fortney JL, Wu J, Hazen TC. 2016. Rapid detection of microbial cell abundance in aquatic systems. Biosensors and Bioelectronics 85:915-923.
23. Qin Y, Hou J, Deng M, Liu Q, Wu C, Ji Y, He X. 2016. Bacterial abundance and diversity in pond water supplied with different feeds. Scientific Reports 6:35232.
24. Pan D, Nolan J, Williams KH, Robbins MJ, Weber KA. 2017. Abundance and Distribution of Microbial Cells and Viruses in an Alluvial Aquifer. Frontiers in Microbiology 8.
25. McKay DS, Gibson EK, Thomas-Keprta KL, Vali H, Romanek CS, Clemett SJ, Chillier XDF, Maechling CR, Zare RN. 1996. Search for Past Life on Mars: Possible Relic Biogenic Activity in Martian Meteorite ALH84001. Science 273:924-930.
26. Luef B, Frischkorn KR, Wrighton KC, Holman H-YN, Birarda G, Thomas BC, Singh A, Williams KH, Siegerist CE, Tringe SG, Downing KH, Comolli LR, Banfield JF. 2015. Diverse uncultivated ultra-small bacterial cells in groundwater. Nature Communications 6:6372.
27. Uwins Philippa JR, Webb Richard I, Taylor Anthony P. 1998. Novel nano-organisms from Australian sandstones, vol 83, p 1541.
28. Lynch M. 2006. Streamlining and simplification of microbial genome architecture. Annu Rev Microbiol 60:327-49.
29. Neuenschwander SM, Ghai R, Pernthaler J, Salcher MM. 2017. Microdiversification in genome-streamlined ubiquitous freshwater Actinobacteria. The Isme Journal 12:185.
30. Brewer TE, Handley KM, Carini P, Gilbert JA, Fierer N. 2016. Genome reduction in an abundant and ubiquitous soil bacterium 'Candidatus Udaeobacter copiosus'. Nature Microbiology 2:16198.

641 31. Dolfing J. 2013. Syntrophy in microbial fuel cells. The Isme Journal 8:4.
642 32. Pande S, Kost C. 2017. Bacterial Unculturability and the Formation of
643 Intercellular Metabolic Networks. Trends in Microbiology 25:349-361.
644 33. Morris JJ, Lenski RE, Zinser ER. 2012. The Black Queen Hypothesis: Evolution of
645 Dependencies through Adaptive Gene Loss. mBio 3.
646 34. Giovannoni SJ, Cameron Thrash J, Temperton B. 2014. Implications of
647 streamlining theory for microbial ecology. The Isme Journal 8:1553.
648 35. Petras D, Jarmusch AK, Dorrestein PC. 2017. From single cells to our planet—
649 recent advances in using mass spectrometry for spatially resolved metabolomics.
650 Current Opinion in Chemical Biology 36:24-31.
651 36. Hopwood DA. 2013. Imaging Mass Spectrometry Reveals Highly Specific
652 Interactions between Actinomycetes To Activate Specialized Metabolic Gene
653 Clusters. Mbio 4.
654 37. Fang J, Dorrestein PC. 2014. Emerging mass spectrometry techniques for the
655 direct analysis of microbial colonies. Current Opinion in Microbiology 19:120-
656 129.
657 38. Garbeva P, van Elsas JD, de Boer W. 2012. Draft Genome Sequence of the
658 Antagonistic Rhizosphere Bacterium Serratia plymuthica Strain PRI-2C. Journal
659 of Bacteriology 194:4119-4120.
660 39. Tyc O, de Jager VCL, van den Berg M, Gerards S, Janssens TKS, Zaagman N, Kai M,
661 Svatos A, Zweers H, Hordijk C, Besselink H, de Boer W, Garbeva P. 2017.
662 Exploring bacterial interspecific interactions for discovery of novel antimicrobial
663 compounds. Microbial Biotechnology 10:910-925.
664 40. de Boer W, Wagenaar AM, Klein Gunnewiek PJA, van Veen JA. 2007. In vitro
665 suppression of fungi caused by combinations of apparently non-antagonistic soil
666 bacteria. Fems Microbiology Ecology 59:177-185.
667 41. Garbeva P, de Boer W. 2009. Inter-specific Interactions Between Carbon-limited
668 Soil Bacteria Affect Behavior and Gene Expression. Microbial Ecology 58:36-46.
669 42. Seemann T. 2014. Prokka: rapid prokaryotic genome annotation. Bioinformatics
670 30:2068-2069.
671 43. Jones P, Binns D, Chang HY, Fraser M, Li W, McAnulla C, McWilliam H, Maslen J,
672 Mitchell A, Nuka G, Pesseat S, Quinn AF, Sangrador-Vegas A, Scheremetjew M,
673 Yong SY, Lopez R, Hunter S. 2014. InterProScan 5: genome-scale protein function
674 classification. Bioinformatics 30:1236-40.
675 44. Medema MH, Blin K, Cimermancic P, de Jager V, Zakrzewski P, Fischbach MA,
676 Weber T, Takano E, Breitling R. 2011. antiSMASH: rapid identification, annotation
677 and analysis of secondary metabolite biosynthesis gene clusters in bacterial and
678 fungal genome sequences. Nucleic Acids Research 39:W339-46.
679 45. Langmead B, Salzberg SL. 2012. Fast gapped-read alignment with Bowtie 2. Nat
680 Meth 9:357-359.
681 46. Li B, Dewey CN. 2011. RSEM: accurate transcript quantification from RNA-Seq
682 data with or without a reference genome. Bmc Bioinformatics 12:1-16.
683 47. Robinson MD, McCarthy DJ, Smyth GK. 2010. edgeR: a Bioconductor package for
684 differential expression analysis of digital gene expression data. Bioinformatics 26.
685 48. Zhou XB, Lindsay H, Robinson MD. 2014. Robustly detecting differential
686 expression in RNA sequencing data using observation weights. Nucleic Acids
687 Research 42.
688 49. Team RC. 2014. R: A language and environment for statistical computing. R
689 Foundation for Statistical Computing, Vienna, Austria. 2013.

690 50. Kanehisa M, Sato Y, Morishima K. 2016. BlastKOALA and GhostKOALA: KEGG
691 Tools for Functional Characterization of Genome and Metagenome Sequences. J
692 Mol Biol 428:726-731.
693 51. Sayers EW, Cavanaugh M, Clark K, Ostell J, Pruitt KD, Karsch-Mizrachi I. 2018.
694 GenBank. Nucleic Acids Research 47:D94-D99.
695 52. Aziz RK, Bartels D, Best AA, DeJongh M, Disz T, Edwards RA, Formsma K, Gerdes
696 S, Glass EM, Kubal M, Meyer F, Olsen GJ, Olson R, Osterman AL, Overbeek RA,
697 McNeil LK, Paarmann D, Paczian T, Parrello B, Pusch GD, Reich C, Stevens R,
698 Vassieva O, Vonstein V, Wilke A, Zagnitko O. 2008. The RAST Server: Rapid
699 Annotations using Subsystems Technology. BMC Genomics 9:75.
700 53. Overbeek R, Olson R, Pusch GD, Olsen GJ, Davis JJ, Disz T, Edwards RA, Gerdes S,
701 Parrello B, Shukla M, Vonstein V, Wattam AR, Xia F, Stevens R. 2014. The SEED
702 and the Rapid Annotation of microbial genomes using Subsystems Technology
703 (RAST). Nucleic Acids Research 42:D206-D214.
704 54. Brettin T, Davis JJ, Disz T, Edwards RA, Gerdes S, Olsen GJ, Olson R, Overbeek R,
705 Parrello B, Pusch GD, Shukla M, Thomason JA, 3rd, Stevens R, Vonstein V, Wattam
706 AR, Xia F. 2015. RASTtk: a modular and extensible implementation of the RAST
707 algorithm for building custom annotation pipelines and annotating batches of
708 genomes. Sci Rep 5:8365.
709 55. Kanehisa M, Sato Y, Kawashima M, Furumichi M, Tanabe M. 2016. KEGG as a
710 reference resource for gene and protein annotation. Nucleic Acids Research
711 44:D457-D462.
712 56. Anonymous. !!! INVALID CITATION !!!
713 57. Muñiz S, Lacarta J, Pata MP, Jiménez JJ, Navarro E. 2014. Analysis of the Diversity
714 of Substrate Utilisation of Soil Bacteria Exposed to Cd and Earthworm Activity
715 Using Generalised Additive Models. PLOS ONE 9:e85057.
716 58. Rutgers M, Wouterse M, Drost SM, Breure AM, Mulder C, Stone D, Creamer RE,
717 Winding A, Bloem J. 2016. Monitoring soil bacteria with community-level
718 physiological profiles using Biolog™ ECO-plates in the Netherlands and Europe.
719 Applied Soil Ecology 97:23-35.
720 59. Garbeva P, Hordijk C, Gerards S, de Boer W. 2014. Volatiles produced by the
721 mycophagous soil bacterium Collimonas. Fems Microbiology Ecology 87.
722 60. Gibb S, Strimmer K. 2012. MALDIquant: a versatile R package for the analysis of
723 mass spectrometry data. Bioinformatics 28:2270-1.
724 61. Bardou P, Mariette J, Escudié F, Djemiel C, Klopp C. 2014. jvenn: an interactive
725 Venn diagram viewer. BMC Bioinformatics 15:293.
726 62. Xia J, Sinelnikov IV, Han B, Wishart DS. 2015. MetaboAnalyst 3.0-making
727 metabolomics more meaningful. Nucleic Acids Research 43:W251-7.
728 63. Hylemon PB, Wells JS, Krieg NR, Jannasch HW. 1973. The Genus Spirillum: a
729 Taxonomic Study1. International Journal of Systematic and Evolutionary
730 Microbiology 23:340-380.
731 64. Pawlowsk D, Raslawsky A, Siebert G, Metzger D, Koudelka G. 2011. Identification
732 of Hylemonella gracilis as an Antagonist of Yersinia pestis Persistence. J Bioterr
733 Biodef S 3:2.
734 65. Spring S, Jackel U, Wagner M, Kampfer P. 2004. Ottowia thiooxydans gen. nov., sp.
735 nov., a novel facultatively anaerobic, N2O-producing bacterium isolated from
736 activated sludge, and transfer of Aquaspirillum gracile to Hylemonella gracilis
737 gen. nov., comb. nov. Int J Syst Evol Microbiol 54:99-106.
738 66. Willems A. 2014. The Family Comamonadaceae, p 777-851. *In* Rosenberg E,
739 DeLong EF, Lory S, Stackebrandt E, Thompson F (ed), The Prokaryotes:

740 Alphaproteobacteria and Betaproteobacteria doi:10.1007/978-3-642-30197-
741 1_238. Springer Berlin Heidelberg, Berlin, Heidelberg.
742 67. Wang Y, Hammes F, Boon N, Egli T. 2007. Quantification of the filterability of
743 freshwater bacteria through 0.45, 0.22, and 0.1 µm pore size filters and shape-
744 dependent enrichment of filterable bacterial communities. Environmental
745 science & technology 41:7080-7086.
746 68. Cobo-Simón M, Tamames J. 2017. Relating genomic characteristics to
747 environmental preferences and ubiquity in different microbial taxa. BMC
748 Genomics 18:499.
749 69. Angly FE, Willner D, Prieto-Davó A, Edwards RA, Schmieder R, Vega-Thurber R,
750 Antonopoulos DA, Barott K, Cottrell MT, Desnues C, Dinsdale EA, Furlan M,
751 Haynes M, Henn MR, Hu Y, Kirchman DL, McDole T, McPherson JD, Meyer F, Miller
752 RM, Mundt E, Naviaux RK, Rodriguez-Mueller B, Stevens R, Wegley L, Zhang L,
753 Zhu B, Rohwer F. 2009. The GAAS Metagenomic Tool and Its Estimations of Viral
754 and Microbial Average Genome Size in Four Major Biomes. PLOS Computational
755 Biology 5:e1000593.
756 70. Frank JA, Sørensen SJ. 2011. Quantitative Metagenomic Analyses Based on
757 Average Genome Size Normalization. Applied and Environmental Microbiology
758 77:2513-2521.
759 71. Xia LC, Cram JA, Chen T, Fuhrman JA, Sun F. 2011. Accurate Genome Relative
760 Abundance Estimation Based on Shotgun Metagenomic Reads. PLOS ONE
761 6:e27992.
762 72. Lee GW, Lee S, Chung MS, Jeong YS, Chung BY. 2015. Rice terpene synthase 20
763 (OsTPS20) plays an important role in producing terpene volatiles in response to
764 abiotic stresses. Protoplasma 252:997-1007.
765 73. Loreto F, Schnitzler J-P. 2010. Abiotic stresses and induced BVOCs. Trends in
766 Plant Science 15:154-166.
767 74. Heng NCK, Wescombe PA, Burton JP, Jack RW, Tagg JR. 2007. The diversity of
768 bacteriocins in Gram-positive bacteria. *In* Riley MA, Chavan MA (ed),
769 Bacteriocins: ecology and evolution. Springer, Berlin.
770 75. Riley MA. 2011. Bacteriocin-mediated competitive interactions of bacterial
771 populations and communities, p 13-26, Prokaryotic Antimicrobial Peptides.
772 Springer.
773 76. Riley MA, Wertz JE. 2002. Bacteriocins: evolution, ecology, and application.
774 Annual Review of Microbiology 56.
775 77. Wadhams GH, Armitage JP. 2004. Making sense of it all: bacterial chemotaxis.
776 Nature reviews Molecular cell biology 5:1024.
777 78. Szurmant H, Ordal GW. 2004. Diversity in chemotaxis mechanisms among the
778 bacteria and archaea. Microbiol Mol Biol Rev 68:301-319.
779 79. Garbeva P, Silby MW, Raaijmakers JM, Levy SB, Boer W. 2011. Transcriptional
780 and antagonistic responses of Pseudomonas fluorescens Pf0-1 to
781 phylogenetically different bacterial competitors. ISME Journal 5:973-85.
782 80. Johnson DC, Dean DR, Smith AD, Johnson MK. 2005. Structure, function, and
783 formation of biological iron-sulfur clusters. Annu Rev Biochem 74:247-81.
784 81. Bandyopadhyay S, Chandramouli K, Johnson MK. 2008. Iron-sulfur cluster
785 biosynthesis. Biochem Soc Trans 36:1112-9.
786 82. Crowley D, Wang Y, Reid C, Szaniszlo P. 1991. Mechanisms of iron acquisition
787 from siderophores by microorganisms and plants, p 213-232, Iron Nutrition and
788 Interactions in Plants. Springer.

83. Allison SD. 2005. Cheaters, diffusion and nutrients constrain decomposition by microbial enzymes in spatially structured environments. Ecology Letters 8:626-635.
84. Pagès A, Grice K, Vacher M, Welsh DT, Teasdale PR, Bennett WW, Greenwood P. 2014. Characterizing microbial communities and processes in a modern stromatolite (S hark B ay) using lipid biomarkers and two - dimensional distributions of porewater solutes. Environmental microbiology 16:2458-2474.
85. Lill R. 2009. Function and biogenesis of iron–sulphur proteins. Nature 460:831.
86. Ishige T, Krause M, Bott M, Wendisch VF, Sahm H. 2003. The Phosphate Starvation Stimulon of Corynebacterium glutamicum Determined by DNA Microarray Analyses. Journal of Bacteriology 185:4519-4529.
87. Picard F, Loubière P, Girbal L, Cocaign-Bousquet M. 2013. The significance of translation regulation in the stress response. Bmc Genomics 14:1-11.
88. Silberbach M, Burkovski A. 2006. Application of global analysis techniques to Corynebacterium glutamicum: New insights into nitrogen regulation. Journal of Biotechnology 126:101-110.
89. Takeuchi O, Sato S, Horiuchi T, Hoshino K, Takeda K, Dong Z, Modlin RL, Akira S. 2002. Cutting edge: role of Toll-like receptor 1 in mediating immune response to microbial lipoproteins. The Journal of Immunology 169:10-14.
90. Hemmi H, Takeuchi O, Kawai T, Kaisho T, Sato S, Sanjo H, Matsumoto M, Hoshino K, Wagner H, Takeda K. 2000. A Toll-like receptor recognizes bacterial DNA. Nature 408:740.
91. Hayashi F, Smith KD, Ozinsky A, Hawn TR, Eugene CY, Goodlett DR, Eng JK, Akira S, Underhill DM, Aderem A. 2001. The innate immune response to bacterial flagellin is mediated by Toll-like receptor 5. Nature 410:1099.
92. Müller V. 2001. Bacterial fermentation. e LS.
93. Muñoz - Elías EJ, McKinney JD. 2006. Carbon metabolism of intracellular bacteria. Cellular microbiology 8:10-22.
94. Huynen MA, Dandekar T, Bork P. 1999. Variation and evolution of the citric-acid cycle: a genomic perspective. Trends in microbiology 7:281-291.
95. Beck HC, Hansen AM, Lauritsen FR. 2003. Novel pyrazine metabolites found in polymyxin biosynthesis by Paenibacillus polymyxa. Fems Microbiology Letters 220:67-73.
96. Kucerova-Chlupacova M, Kunes J, Buchta V, Vejsova M, Opletalova V. 2015. Novel pyrazine analogs of chalcones: synthesis and evaluation of their antifungal and antimycobacterial activity. Molecules 20:1104-17.
97. Lapenda J, Silva P, Vicalvi M, Sena K, Nascimento S. 2015. Antimicrobial activity of prodigiosin isolated from Serratia marcescens UFPEDA 398. World Journal of Microbiology and Biotechnology 31:399-406.
98. Chernin L, Brandis A, Ismailov Z, Chet I. 1996. Pyrrolnitrin production by an Enterobacter agglomerans strain with a broad spectrum of antagonistic activity towards fungal and bacterial phytopathogens. Current Microbiology 32:208-212.
99. Dhar Purkayastha G, Mangar P, Saha A, Saha D. 2018. Evaluation of the biocontrol efficacy of a Serratia marcescens strain indigenous to tea rhizosphere for the management of root rot disease in tea. PloS one 13:e0191761-e0191761.
100. Kulkarni P, Wilschut RA, Verhoeven KJ, van der Putten WH, Garbeva P. 2018. LAESI mass spectrometry imaging as a tool to differentiate the root metabolome of native and range-expanding plant species. Planta 248:1515-1523.

101. Li H, Smith BK, Márk L, Nemes P, Nazarian J, Vertes A. 2015. Ambient molecular imaging by laser ablation electrospray ionization mass spectrometry with ion mobility separation. International Journal of Mass Spectrometry 377:681-689.
102. Stopka SA, Agtuca BJ, Koppenaal DW, Paša - Tolić L, Stacey G, Vertes A, Anderton CR. 2017. Laser - ablation electrospray ionization mass spectrometry with ion mobility separation reveals metabolites in the symbiotic interactions of soybean roots and rhizobia. The Plant Journal 91:340-354.
103. Schulz S, Fuhlendorff J, Reichenbach H. 2004. Identification and synthesis of volatiles released by the myxobacterium Chondromyces crocatus. Tetrahedron 60:3863-3872.
104. Blom D, Fabbri C, Connor EC, Schiestl FP, Klauser DR, Boller T, Eberl L, Weisskopf L. 2011. Production of plant growth modulating volatiles is widespread among rhizosphere bacteria and strongly depends on culture conditions. Environmental Microbiology 13:3047-3058.
105. Kabil O, Vitvitsky V, Banerjee R. 2014. Sulfur as a signaling nutrient through hydrogen sulfide. Annual review of nutrition 34:171-205.
106. Audrain B, Farag MA, Ryu CM, Ghigo JM. 2015. Role of bacterial volatile compounds in bacterial biology. Fems Microbiology Reviews 39:222-233.

Table 1: Genome assembly statistics and outcome of the *in silico* analysis on secondary metabolite gene clusters of *H. gracilis, Serratia plymuthica* PRI-2C and *Paenibacillus* sp. AD87.

Feature / Organism	***Hylemonella gracilis***	***S. plymuthica* PRI-2C**	***Paenibacillus* sp. AD87**
contigs	1	1	30
bases	3822245	5474685	7086713
number of chromosomes	1	1	1
size chromosome 1	3822245	5464425	7086713
CDS	3648	4929	6216
GC- content (%)	65.1	55.7	46.2
number of RNAs	53	109	146
genes	3625	5284	6375
in silico detected secondary metabolite clusters (antiSMASH)	3	9	10
Total genome size (bases)	**3822245**	**5474685**	**7086713**

Table 2: Tentatively identified volatile organic compounds (VOCs) produced by a *H. gracilis, Serratia plymuthica* PRI-2C and *Paenibacillus* sp. AD87 strains in mono- and co-cultures.

#	Compound name	RT*	ELRI**	p-value***	chemical class	Detected in treatment				
						HM	SM	SH	PM	PH
1	2-methylfuran	2,18	738	0,041	Furan	X		X	X	X
2	2-methylpropanoic Acid	3,01	755	0,014	Alkenes	X	X	X	X	X
3	mix pentanal + heptane	3,21	760	0,008	Alkenes	X		X		X
4	methyl thycocyanate	3,44	764	0,020	Thioesters	X	X	X	X	X
5	1-Pentanol	3,95	772	0,012	Alkenes		X	X	X	X
6	dimethyl disulfide	4,01	775	0,012	Sulfides	X	X	X	X	X
7	unknown compound 1	4,15	778	0,003	-		X	X	X	
8	toluene	4,44	784	0,014	Benzenoids	X	X	X	X	X
9	methyl Isovalerate	4,76	789	0,018	Terpenes		X	X	X	X
10	cyclohexane	8,07	852	0,031	Alkenes		X	X	X	X
11	dimethyl trisulfide	11,35	914	0,013	Sulfides	X	X	X	X	X
12	benzonitrilie	12,06	928	0,037	Alkenes	X	X	X	X	X
13	2-Ethyl-4-methylpentan-1-ol	17,26	1026	0,015	Alkenes		X	X	X	X
14	2,5-bis(1-methylethyl)-pyrazine	20,56	1090	0,031	Pyrazines				X	X
15	undecane	21,31	1100	0,014	Alkenes	X		X	X	X
16	unknown compound 2	24,34	1140	0,013	-				X	
17	unknown compound 3	25,92	1160	0,011	-	X	X	X	X	X
19	unknown compound 4	26,40	1165	0,018	-	X		X	X	X
20	unknown compound 5	26,90	1170	0,003	-	X			X	X
21	alpha-terpineol	27,34	1178	0,016	Terpenes	X	X	X	X	X
22	undecane, 2,6-dimethyl	28,27	1190	0,004	Benzenoids	X	X	X	X	X
23	gamma-terpineol	28,42	1192	0,006	Terpenes	X		X		
24	terpene like compound 1	29,32	1202	0,012	Terpenes	X		X		
25	terpene like compound 2	31,49	1231	0,009	Terpenes	X	X	X	X	X
Number of detected compounds (n)						**16**	**15**	**20**	**20**	**19**

Abbreviations:

HM= *H. gracilis* monoculture, SM= *Serratia plymuthica* PRI-2C monoculture, PM= *Paenibacillus* sp. AD87 monoculture, PH= *Paenibacillus* sp. AD87 and *H. gracilis* co-culture, SH= *Serratia plymuthica* PRI-2C and *H. gracilis* co-culture

= Compound number

RT* = Retention time, the RT value stated is the average of three technical replicates.

ELRI** = Experimental linear retention index value, the RI value stated is the average of three replicates.

p-value***= statistical significance (peak area and peak intensity)

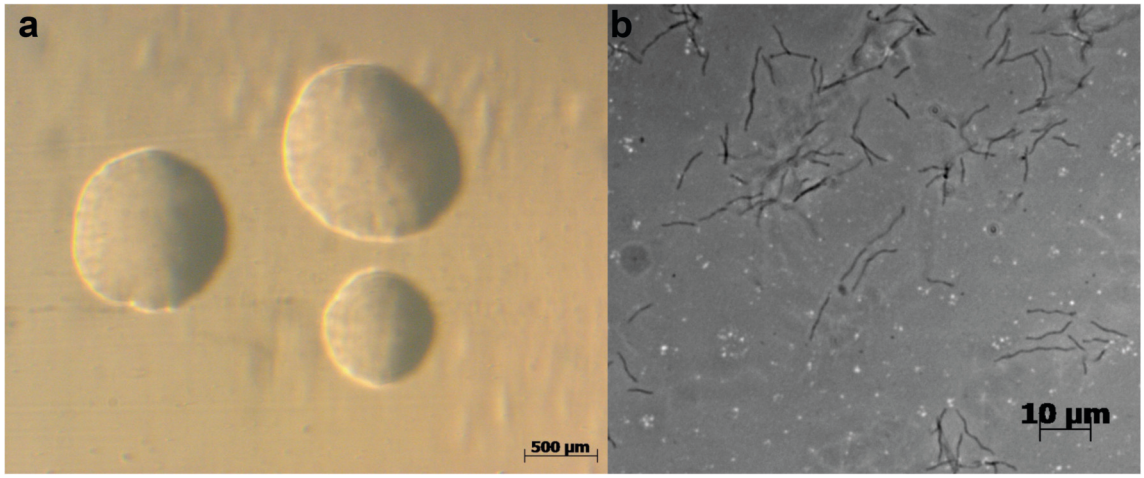

Figure 1: Microscopy pictures of *Hylemonella gracilis* (**a**) colonies on agar plates captured at 20x magnification and (**b**) single bacterial cells captured at 400 X magnification.

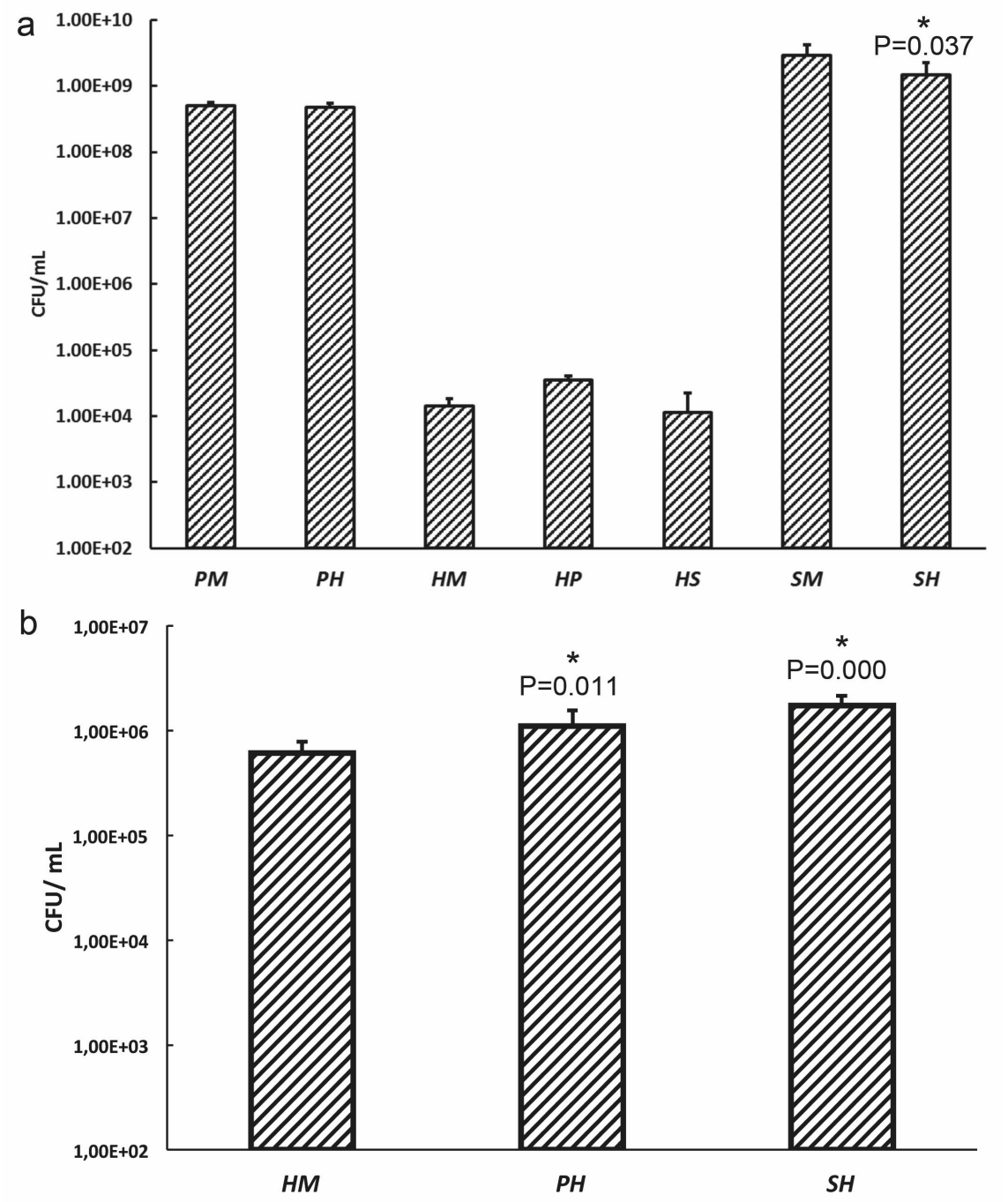

Figure 2: Colony counts (CFU/mL) revealed after 5 days of incubation during the plate based interaction experiment (a) and (b) revealed during the cell free supernatant (CFS) exposure experiment. Abbreviations: *H. gracilis* monoculture (HM), *Paenibacillus* sp. AD87 monoculture (PM), *Paenibacillus* sp. AD87 – *H. gracilis* coculture (PH), *S. plymuthica* monoculture (SM), *S. plymuthica* - *H. gracilis* coculture (SH). *H. gracilis* - *Paenibacillus* sp. AD87 coculture (HP), *H. gracilis* – *S. plymuthica* coculture (HS). Significant differences in cell counts (CFU/mL) between co-cultures (treatment) and monocultures (controls) are indicated by asterisks (ONE-WAY ANOVA, post-hoc TUKEY test).

Strain/Treatment	*PM*	SM	*HM*	*PH*	*SH*
Compound					
Pyruvic Acid Methyl Ester					
Tween 40					
Tween 80					
α-Cyclodextrin					
Glycogen					
D-Cellobiose					
α-D-Lactose					
β-Methyl-D-Glucoside					
D-Xylose					
i-Erythritol					
D-Mannitol					
N-Acetyl-D-Glucosamine					
D-Glucosaminic Acid					
Glucose-1-Phosphate					
D-L-α-Glycerol Phosphate					
D-Galactonic Acid γ-Lactone					
D-Galacturonic Acid					
2-Hydroxy Benzoic Acid					
4-Hydroxy Benzoic Acid					
γ-Hydroxybutyric Acid					
Lactonic Acid					
α-Ketobutyric Acid					
D-Malic Acid					
L-Arginine					
L-Asparagine					
L-Phenylalanine					
L-Serine					
L-Threonine					
Glycyl-L-Glutamic Acid					
Phenylethyl-amine					
Putrescine					

Figure 3: Results overview of the Biolog EcoPlate™ experiment. The EcoPlate contains 31 different carbon sources, bacteria were inoculated in monoculture or in pairwise combinations. Colour codec: blue=carbon source could be utilized in monoculture, yellow= carbon source could be utilized in co-culture. Abbreviations: *Paenibacillus* sp. AD87 monoculture (PM), *Paenibacillus* sp. AD87 - *H. gracilis* coculture, (PH) *H. gracilis* monoculture (HM), *S. plymuthica* PRI-2C monoculture (SM), *S. plymuthica* PRI-2C - *H. gracilis* coculture (SH).

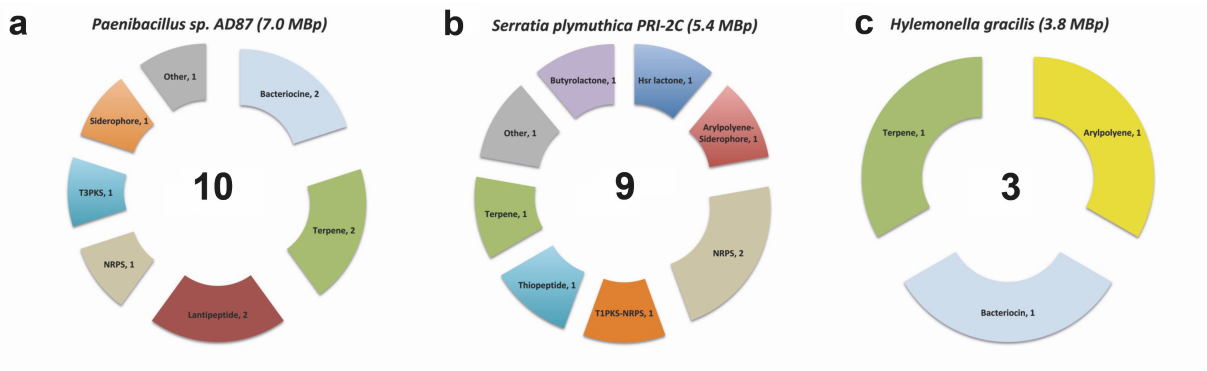

Figure 4: *In silio* comparison of biosynthetic gene clusters (BGCs) present in the three soil bacteria based on antismash *in silico* analysis (https://antismash.secondarymetabolites.org/). From left to right (**a**) *Paenibacillus* sp. AD87 with a genome size of 7.0 MBp, n=10 gene clusters for secondary metabolites, (**b**) *S. plymuthica* PRI-2C with a genome size of 5.4 MBp, n=9 gene clusters for secondary metabolites and (**c**) *H. gracilis* with a genome size of 3.8 MBp, n= 3 gene clusters for secondary metabolites.

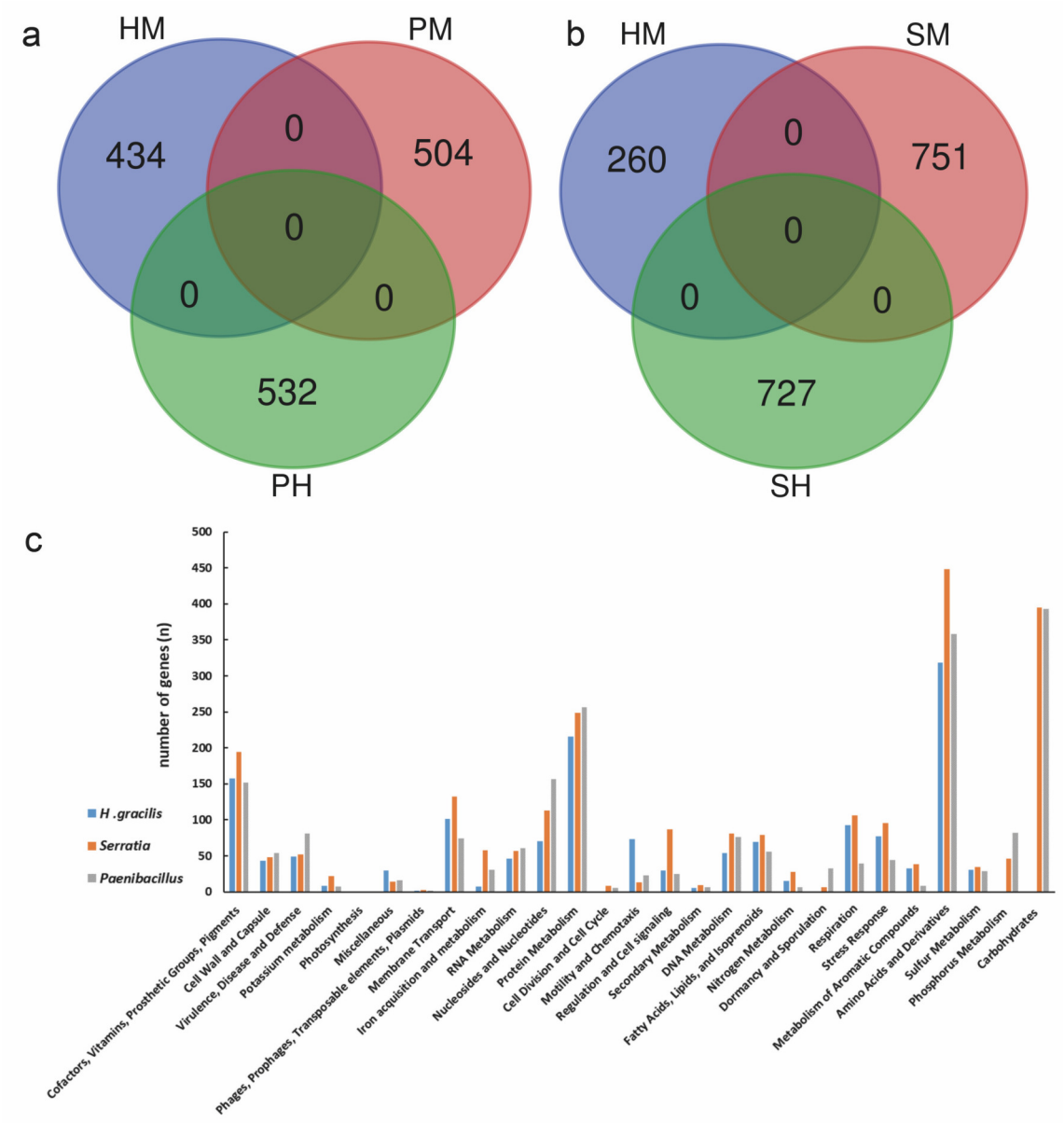

Figure 5: Results of the comparison analysis carried out with the RAST pipeline (https://rast.nmpdr.org/) (**a**) Venn- diagram showing the results for the number (n) of expressed genes present solely in monoculture and the number of shared expressed genes for the monocultures of *Hylemonella* (HM), *Paenibacillus* monoculture (PM) and *Serratia* monoculture (SM) and the interaction of *Hylemonella* with *Paenibacillus* (PH) and for the interaction of *Hylemonella* with *Serratia* (SH). (**b**) Boxplot showing number (n) of expressed genes present in each RAST subsystem category.

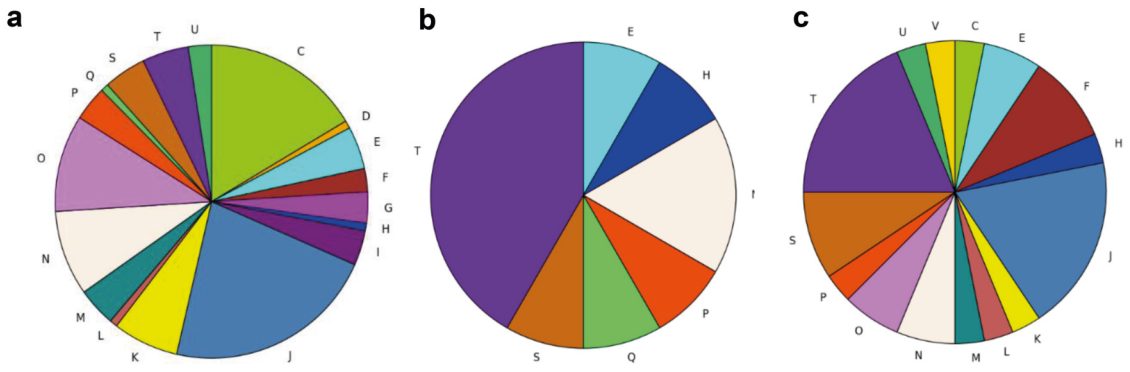

Figure 6: Pie-charts representing up-regulated genes identified by differential gene expression analysis and COG annotation (**a**) *Hylemonella gracilis* monoculture gene expression level (**b**) *H. gracilis* in co-culture with *Paenibacillus* sp. AD87; (**c**) *H. gracilis* co-culture with *S. plymuthica* PRI-2C. In the co-culture of *H. gracilis* with *Paenibacillus* sp. AD87, genes related to signal transduction (**T**) were the category with the most differentially expressed genes. In the co- culture of *H. gracilis* with *S. plymuthica* PRI-2C genes related to signal transduction (**T**), translation, ribosome structure and biogenesis (**J**) were the most prevalent differentially expressed gene categories.

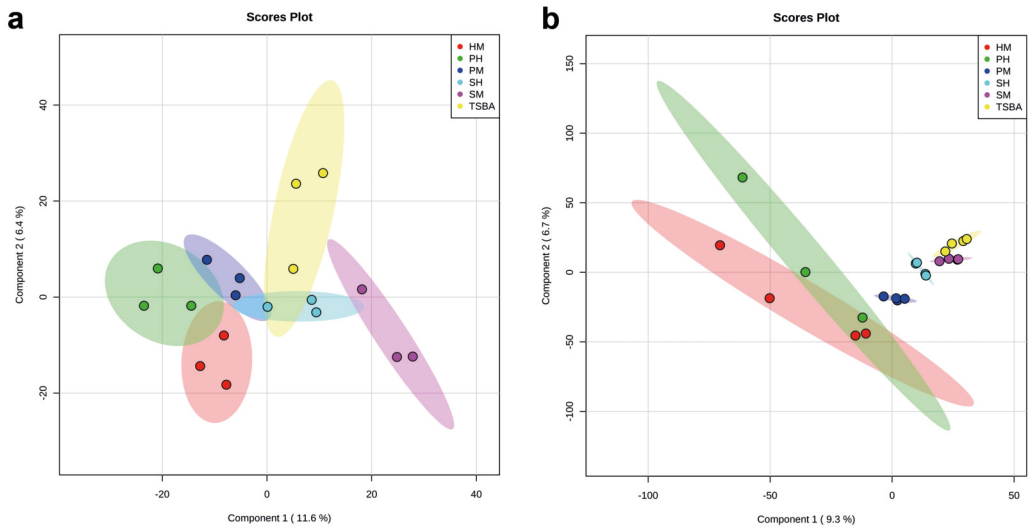

Figure 7: PLSD-A plots of the metabolomics data (**a**) PLS-DA 2D- plots of volatiles emitted by monocultures and pairwise combinations of *H. gracilis*, *Paenibacillus* and *Serratia plymuthica* after ten days of inoculation, time point (t=10 days) (**b**) PLS-DA 2D- plots of the analysed DART-MS data of monocultures and mixtures of *H. gracilis*, *Paenibacillus* sp. AD87 and *Serratia plymuthica* PRI-2C after ten days of inoculation, time point (t=10 days).

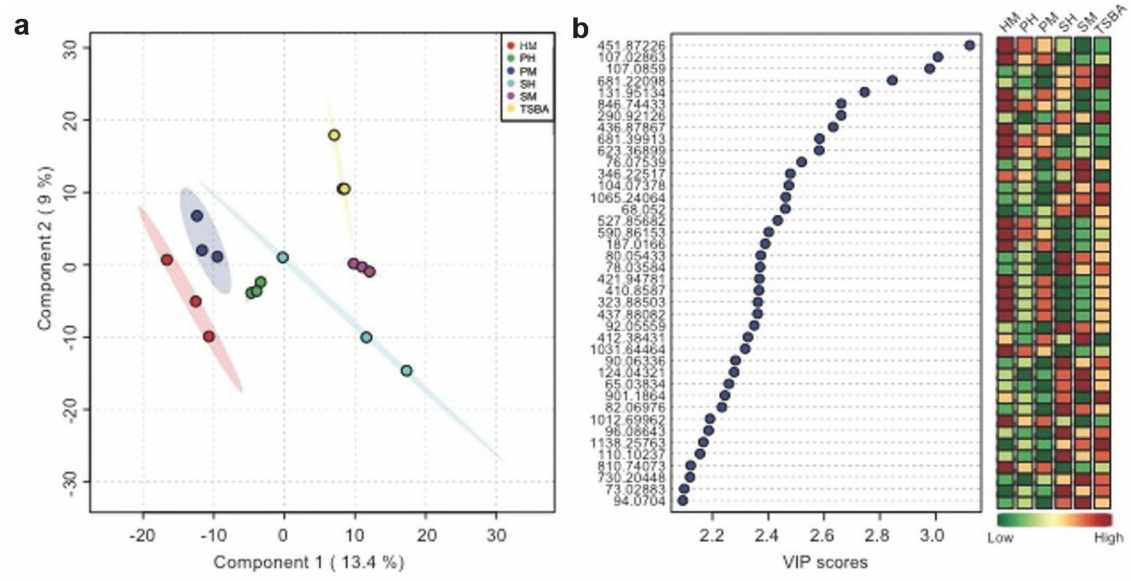

Figure 8: PLS-DA plots of the first 40 significant mass features observed after analysis of the LAESI-MSI data. (a) PLS-DA score plot for *H. gracilis* monoculture (HM), *Paenibacillus sp. AD87* monoculture (PM), *Paenibacillus* sp. AD87 – *H. gracilis* coculture (PH), *S. plymuthica* PRI-2C monoculture (SM), *S. plymuthica* PRI-2C - *H. gracilis* coculture (SH) and TSBA control (TSBA). **(b)** First 40 statistically significant features identified by PLS-DA based on Variable Importance in Projection (VIP) score. The colored boxes on the right indicate the relative concentrations of the corresponding metabolite in each group under study.